UCRL-9321

UNIVERSITY OF CALIFORNIA

Ernest O. Lawrence Radiation Laboratory

TWO-WEEK LOAN COPY

This is a Library Circulating Copy which may be borrowed for two weeks. For a personal retention copy, call Tech. Info. Division, Ext. 5545

BERKELEY, CALIFORNIA

DISCLAIMER

This document was prepared as an account of work sponsored by the United States Government. While this document is believed to contain correct information, neither the United States Government nor any agency thereof, nor the Regents of the University of California, nor any of their employees, makes any warranty, express or implied, or assumes any legal responsibility for the accuracy, completeness, or usefulness of any information, apparatus, product, or process disclosed, or represents that its use would not infringe privately owned rights. Reference herein to any specific commercial product, process, or service by its trade name, trademark, manufacturer, or otherwise, does not necessarily constitute or imply its endorsement, recommendation, or favoring by the United States Government or any agency thereof, or the Regents of the University of California. The views and opinions of authors expressed herein do not necessarily state or reflect those of the United States Government or any agency thereof or the Regents of the University of California.

UCRL-9321
Limited Distribution

UNIVERSITY OF CALIFORNIA
Lawrence Radiation Laboratory
Berkeley, California

Contract No. W-7405-eng-48

FISSION THRESHOLDS FOR ELEMENTS LIGHTER THAN RADIUM

Donald S. Burnett and Stanley G. Thompson

July 25, 1960

FISSION THRESHOLDS FOR ELEMENTS

LIGHTER THAN RADIUM

Contents

Page

Abstract 3

Introduction 4

I. Definition of a Fission Threshold 6

II. Estimation of Thresholds from Γ_f/Γ_n Values 15

III. Semi-Empirical Liquid Drop Estimation of Fission Thresholds 25

Conclusion 28

Acknowledgment 34

Appendix 35
Correlation of Γ_f/Γ_n Data with Other Paramenters

References 39

FISSION THRESHOLDS FOR ELEMENTS LIGHTER THAN RADIUM

Donald S. Burnett and Stanley G. Thompson

Lawrence Radiation Laboratory
University of California
Berkeley, California

July 25, 1960

ABSTRACT

Semiempirical considerations based on already existing data are employed to estimate values for the fission thresholds in the elements ranging from Ta to Ra.

Threshold values are obtained in two ways: (a) From interpretation of experimental fission cross-section measurements by means of the Fujimoto-Yamaguchi expression for $\Gamma f/\Gamma n$, and (b) by an approximate liquid-drop equation that expresses the saddle-point mass as a function of the fissionability parameter, x. A compilation of the experimental fission cross-section data for light elements available at the time of writing is included.

FISSION THRESHOLDS FOR ELEMENTS LIGHTER THAN RADIUM*

Donald S. Burnett and Stanley G. Thompson

Lawrence Radiation Laboratory
University of California
Berkeley, California

July 25, 1960

INTRODUCTION

Current trends suggest that the fission process is significantly different in the lower elements than in the elements of $Z > 90$. First, the most striking evidence is the change in the mass-yield curves. From predominantly asymmetric fission at uranium and thorium the yield of the symmetric mode increases abruptly, giving a three-humped peak at radium[1] followed by complete symmetric distributions for lead and bismuth.[2] (However, see Reference 13.) For example, the fission of Th^{229}, differing by only 2 units of Z and A from Ra^{227}, is asymmetric.[3] Second, the decline of fission as a competing mode in nuclear reactions at moderate energies occurs abruptly at the region of radium. This suggests that the fission barrier heights, which are approximately constant for the elements of $Z > 90$, have undergone a sharp increase in the lighter elements. This increase in threshold is to be expected according to the liquid-drop model, and current calculations indicate that this model may account for the over-all changes in the process in this region of the periodic table. At present the information available from theory and experiment are insufficient to give unambiguous answers to these questions.

The location of the change in the characteristics of the fission process at radium is not inconsistent with the result of liquid-drop calculations, since it was at about this value of the fissility parameter that the change in the saddlepoint shapes of the Frankel and Metropolis calculations[4] occurred. The current calculations[5] indicate that in this region the barrier changes from two peaks with a flat minimum or "puddle" between them to only one peak, but with a rather gradual slope along a path from the undeformed configuration to the saddle. Estimates of the threshold for various equilibrium shapes for

---

* This work was performed under the auspices of the U.S. Atomic Energy Commission.

low values of x have indicated that the behavior is other than that which would be expected if the limiting $(1-x)^3$ threshold merely changed in some smooth gradual way to reach its proper intercept at x=0, i.e., the threshold as a function of x has at least two distinct regions, the $(1-x)^3$ region, and a second region about which more will be said later; furthermore a change-over between these regions at about Ra would not present a too unreasonable picture.

The investigation of what is known, or can be said of the threshold behavior of elements for which fission cross sections are measurable but do not fall within the range of the $(1-x)^3$ law will be the concern of this paper.

I. DEFINITION OF A FISSION THRESHOLD

The usual definition of the threshold of a nuclear reaction is "the lowest energy of incident particle (or excitation energy) at which a reaction becomes energetically possible," i.e., the concept is usually applied only to "endothermic" processes. Fission becomes exothermic at about zirconium and becomes more and more energetically favorable as the number of nucleons increases beyond this; consequently on this basis we would not expect fission to show a true threshold any more than we would expect it to be exhibited in a process such as alpha decay. The question then is: how can we make an operational definition of a fission threshold? In other words, (a) what empirical measurements are required, and (b) by what manner must they be assembled or combined? The definition must include criteria for the determination of answers to these two questions. We must keep this in mind when we consider the accepted meaning of a fission threshold.

The threshold is usually considered to be that excitation energy at which the process ceases to be one of barrier penetration; i.e., the fission threshold is identical with the height of the fission barrier. This is an extremely convenient definition to use in conjunction with theoretical or semiempirical calculations, since the barrier height would be an important consequence of any proposed model of the fission process. One way to define a fission barrier in terms of observable quantities is to rely on equations derived from various models that contain the barrier height as an undetermined parameter related to other directly measured or calculable quantities. By fitting appropriate experimental data to this equation we can hope to obtain a value for the barrier height. This is the principal approach of this paper, however, it is an approach more of necessity than of choice. Interpretation of data or estimation of physical quantities by means of a model can be no more accurate than the model itself. Any measurable change in the properties of a system that is coincident with the attainment of the barrier height is preferable to estimation from a model as a means of determining a threshold. A simple qualitative argument can be used to show that such an effect may exist.

The change referred to is one of the cross section at the barrier; the penetrability of a fission barrier decreases sharply below the top: a change

of a factor about 7.85 powers of 10 per Mev change in excitation energy is estimated by Frankel and Metropolis for x=0.74.[4] Since the cross section is proportional to this penetrability factor, we should expect a corresponding sharp decrease in cross section with excitation energy. Such curves have been observed with the heavier nuclides such as U^{238} and Th^{232}.[6] There the breaks in the excitation function serve to locate the threshold to ±0.5 Mev. Precision such as this would be sufficient for almost all purposes at our present state of knowledge of the fission process in the lighter elements.

But, as noted above, the fission process is different for the light elements. What effect will this have on the above argument? The observed fission cross-section curves rise steeply even at energies suspected to be above the barrier. Reference to Figure 3 will show that the curves for light elements are roughly parallel and, more important, have a change of a factor of approximately ten per 7 Mev of excitation; thus we would still expect a sharp change in slope to mark the fission barrier provided measurements were made at low enough excitation energies. Unfortunately, the experimental problems associated with the measurement of such low cross-sections have been sufficiently difficult that this effect has yet to be observed for light elements (however, see the intepretation of Leachman's Ra data[7] by Vandenbosch,[8] Figure 5b).

A quantitative order-of-magnitude estimate to back up the above qualitative arguments can be made. Liquid-drop calculations[4, 5, 9] have shown that with decreasing x the fission barriers take on shapes as shown in Figure 1. For the purposes of calculation these barriers have been idealized as shown by the dotted lines of Figure 2. For x=0.75 a rectangular approximation has been used, whereas a triangular shape was chosen for x=0.5. The estimation using the triangular barrier should be more significant for the fission of light elements. It should be noted that the triangular idealization is working against the effect we are trying to illustrate, since the actual barrier would be expected to be wider, giving a larger change per Mev in penetrability than the triangle. Nevertheless these estimates must be considered quite crude, because it is very unlikely that any one-dimensional picture of the barrier can represent the physics of the situation. However, since all we wish to show is that there would be a large change in slope of the excitation function at the barrier in the lighter elements, these calculations should be sufficient.

The JWKB expression for the penetration probability, P, of an arbitrarily shaped barrier is

$$\ln p = \frac{-2}{\hbar} \int_{\text{barrier}} \sqrt{2 M_e (V-E_x)} \; du, \qquad (1)$$

where E_x is the excitation energy, u is a coordinate associated with a particular path through the barrier, and V is the potential along this path. M_e must be interpreted as an effective mass such that the kinetic energy associated with the trajectory is $1/2\, M_e\, (du/dt)^2$.

CASE 1. TRIANGULAR BARRIER

As a deformation coordinate let us choose the maximum radius of the deformed shape,

$$R_{max} = R_o(1+a), \qquad (2)$$

and define $\epsilon = (B_f - E_x)$, where B_f is the maximum barrier height; we then have (from Figure 2),

$$\epsilon/L = B_f/aR_o = y/u, \qquad (3)$$
$$y = (V-E_x).$$

Since we are considering the behavior of cross-sections just below the barrier, i.e., calculating the penetrability near the top of the barrier, we can assume that the nuclear shape is but slightly changed by the nucleus going through, rather than over, the fission barrier. Furthermore, the recent liquid-drop calculations[5] have shown that there is little shift in the deformation coordinates associated with the saddle point in the range of x where the triangular approximation might most nearly apply and that the saddle point shapes differ but slightly from those found by Frankel and Metropolis at x=0.65. We can thus associate the Frankel and Metropolis value of $R_{max} \approx 2.2$ for the critical deformation in the region we are considering. Frankel and Metropolis have also estimated M_e as a function of R_{max}, and for deformations in the neighborhood of $R_{max} \approx 2$ the effective mass is very near the total nuclear mass. Consequently, we can set approximately $M_e = M = M_n A$ where M_n is an average

nucleon mass. All these approximations are valid only because we are restricting our attention to the change in cross-section near the top of the barrier.

Combining Eq. (3) and Eq. (1) we obtain

$$\ln p = -\frac{2}{\hbar}\int_0^L \sqrt{2M\left(B_f/a\,R_o\right)u}\;du \qquad (4)$$

$$= -\frac{2}{\hbar}\sqrt{2M\,B_f/a\,R_o}\;L^{3/2}\;\frac{2}{3}$$

$$= -\frac{2}{\hbar}\sqrt{2M}\;\frac{3}{2}\;\epsilon^{3/2}\left(\frac{a\,R_o}{B_f}\right).$$

Since the fission cross-section is proportional to p below the barrier we have,

$$\frac{d\log\sigma_f}{d\,E_x} = -\frac{1}{2.303}\frac{d\ln p}{d\epsilon} = \frac{1}{2.303}\frac{2}{\hbar}\sqrt{2M}\;\epsilon^{1/2}\left(\frac{a\,R_o}{B_f}\right) \qquad (5)$$

$$= 0.77\,\epsilon^{1/2},$$

using A=200, $R_o = r_o A^{1/3}$, B_f= 30 Mev, $(2M_n r_o^2/h^2)^{1/2} = 1/(14)^{1/2}\ (\text{Mev})^{-1/2}$.

This gives

ϵ (Mev)	Slope (logarithmic) (Mev^{-1})
0	0
1	0.77
2	1.09
3	1.33

The observed cross-section curves (Figure 3) have a slope of a factor of about ten per 7 Mev, whereas on this model the predicted slope 1 Mev below the barrier is about a factor of ten in 1.3 Mev, i.e., a change in slope by a factor of roughly 5 within 1 Mev would be observed when the barrier is encountered.

CASE 2. RECTANGULAR BARRIER

From Figure 2 and Eq. (1) we have

$$\ln p = -\frac{2}{\hbar}\int_{R_o}^{(1+a)R_o}\sqrt{2M_e\,\epsilon}\;du, \qquad (6)$$

where ϵ is now a constant with respect to changes in u. Since the nuclear shape in this case will not be constant during the penetration of the barrier, M_e cannot be considered a constant, however, a linear approximation to the Frankel and Metropolis curve for M_e vs. the maximum radius can be made as follows:

$$M_e(u) = (0.3 + 0.7\,(U-R_o/aR_o))M = 0.3M\,(1+7/3\,[U-R_o]/aR_o). \quad (7)$$

Thus we have

$$\ln p = -\frac{2}{\hbar}\int_{R_o}^{(1+a)R_o} \sqrt{2M_e\epsilon}\;du = -\frac{2}{\hbar}\sqrt{2\epsilon}\int_{R_o}^{(1+a)R_o} \sqrt{0.3M}\,(1+7/3\left[\frac{u-R_o}{aR_o}\right])^{1/2}\,du. \quad (8)$$

From this equation, using the Frankel and Metropolis value of a = 0.7 at x = 0.74 and the other constants as in Case 1, we obtain

$$\frac{d\log\sigma}{d\,E_x} = -\frac{1}{2.303}\,\frac{d\ln p}{d\epsilon} = \epsilon^{-1/2}\,(5.43) \quad (9)$$

and the values given in the table.

ϵ (Mev)	Slope (logarithmic) (Mev^{-1})
0	∞
1	5.43
2	3.83
3	3.13

Thus in the other limiting case the change in slope at the barrier is still larger. To the extent that these calcutions can be taken seriously, we can expect that a sharp change in the slope of the excitation function should exist in practice and should serve to mark the barrier to within 1 Mev.

We now formulate various equations from which we may make estimates of the fission threshold from experimental data (Part IIA). These are applied (Part IIC) to data collected from the literature (IIB). Finally, in

Part III, these values are compared with a liquid-drop-model calculation suggested by Swiatecki in an attempt to represent the threshold as a function of x for the lighter elements.

II. THRESHOLDS FROM EXPERIMENTAL DATA

A. Estimation of the threshold from Γ_f/Γ_n ratios observed in alpha bombardments.

Assuming alpha-induced fission to be a compound nucleus process, we have

$$\sigma_f = \sigma_c \, \Gamma_f/\Gamma_T,$$

$$\Gamma_T = \Gamma_f + \Gamma_n + \Gamma_p + \Gamma_a + \ldots \quad , \tag{10}$$

where σ_f is the total fission cross-section, σ_c is the cross-section for formation of the compound nucleus, Γ_f is the fission width, and Γ_T is the total reaction width. In dealing with excitation energies of 25 to 30 Mev a good approximation is

$$\Gamma_T = \Gamma_f + \Gamma_n + \Gamma_p + \Gamma_\alpha + \Gamma_\gamma + \ldots \approx \Gamma_n \; . \tag{11}$$

Therefore, since neutron emission is much more highly favored than any other mode of de-excitation, we have

$$\sigma_f \approx \sigma_c \, \Gamma_f/\Gamma_n \; . \tag{12}$$

As σ_c may be calculated theoretically with sufficient precision, the measured σ_f gives values of Γ_f/Γ_n directly. The ordinary expression for the formation of the compound nucleus by charged particles may be used:

$$\sigma_c = \pi \, (R + \lambda\!\!\!^{-})^2 \left(1 - \frac{U}{T'}\right), \tag{13}$$

where R is the radius of the target nucleus ($1.5 \; 10^{-13} \; A^{1/3}$), and T' is the kinetic energy of the alpha particle in the center-of-mass. The value 1.5 for the liquid-drop radius parameter was used, since it was reported to be the value used by Fairhall[2], and the objective was to put new points on his already

existing Γ_f/Γ_n curves. Here, $\lambda\!\!\!^{-}$ is the DeBroglie wave length of the incident alpha in the center-of-mass system, U is the Coulomb barrier height, and

$$U = \frac{Z\ ze^2}{R} \approx 1.92\ Z/A^{1/3} \text{ (in Mev) for alpha particles.} \qquad (14)$$

The formulae, relating Γ_f/Γ_n to the fission barrier, B_f, which have been used [8,10,11] are only slightly different from the original derivation outlined by Fujimoto and Yamaguchi,[12] which in turn was based on the statistical expression given by Bohr and Wheeler[13] for Γ_f and the Fermi gas expression for level density. Fujimoto and Yamaguchi obtain, after considerable approximation,

$$\Gamma_n = 1/2\ \pi\ A^{2/3}/K'\ T^2\ \exp\ (-B_n/T),$$

$$\Gamma_f = 1/2\ T\ \pi\ \exp\ (-B_f/T),$$

$$\Gamma_f/\Gamma_n = 1/T\ K'/A^{2/3}\ \exp\ \left[(B_n-B_f)/T\right], \qquad (15)$$

where K' is $\hbar^2/2mr_o^2$, T is the nuclear temperature, B_n is neutron binding energy, and B_f is the height of the fission barrier.

Huizenga[14] has shown that Eq. (15) is also obtained if a constant nuclear temperature is assumed, and develops the more complete expressions for Γ_f and Γ_n based on the Fermi gas model. Huizenga's expressions reduce to the above in the limit of very high excitation.

Halpern[10] uses a slightly different approach. He adopts only the functional form of the Fujimoto and Yamaguchi expressions,

$$\Gamma_n/\Gamma_f = N\ \exp^{-}\left[(B_n-B_f)/T\right], \qquad (16)$$

where the only requirement on N is that it be a more slowly varying function of excitation E than the exponential. He also derives the exact Fujimoto and Yamaguchi form of the Γ_f/Γ_n expression directly, using statistical arguments based on thermionic emission equations. For actual calculations he tries to fit an equation

$$\Gamma_f/\Gamma_n = 0.6\ \exp\ \left[(B_n-B_f)/T\right], \qquad (17)$$

which he states represents the alpha-induced fission of heavy elements, on the light-element data of Fairhall,[1] and from this to estimate values of B_f. He uses a nuclear temperature expression

$$T^2 = E_x/7.5 \ ,$$

$$E_x = \text{excitation energy (in Mev)}. \qquad (18)$$

He finds that Eq. (17) gives satisfactory qualitative representation to the observed curves and ascribes the differences to the energy dependence of the pre-exponential factor; furthermore the thresholds estimated are roughly what would be expected in view of the increased difficulty of observing the fission process in the lighter elements. He estimates 32 Mev as the threshold for fission produced by alpha bombardments on Pt, 28 for alpha particles on Hg, and 22 for alpha particles on lead.

It was decided to further test the validity of an expression such as

$$\Gamma_f/\Gamma_n = K \exp \left[(B_n - B_f)/T\right] \qquad (19)$$

to handle light-element fission, since further measurements by Fairhall[2] had been carried out and some new data on Re and Ta fission by Griffioen[14] were available, and to utilize them as a means of obtaining estimates of the thresholds from experimental data. The approximations involved in Eqs. (15) to (17) are sufficiently questionable at low excitation energies; consequently attempting to represent the data by an equation like (19) must be considered a somewhat empirical approach. K was assumed, as a first approximation, not to depend on the excitation energy directly; however, no attempt was made to fix it exactly as Halpern had done, i.e., K was allowed to be a function of Z, A, Z^2/A, etc., to say it still another way, we do not demand that all curves have a common intercept as $\sqrt{E_x}$ approaches zero. Writing $T = c\,(E_x)^{1/2}$, where E_x is the excitation energy, we have

$$\log \Gamma_f/\Gamma_n = \log K + \frac{B_n - B_f}{2.303\ c\sqrt{E_x}} \ . \qquad (20)$$

Once c is evaluated (it was chosen to leave this as an adjustable parameter), B_f should be determined by the slope of a plot of $\log \Gamma_f/\Gamma_n$ vs. $1/(E_x)^{1/2}$.

Vandenbosch and Huizenga[8] have constructed a plot of $(B_n - B_f)$ vs. $\log \Gamma_f/\Gamma_n$ for a constant excitation for heavy elements. This curve was used to determine a value of c based on the assumption that an equation of the form of Eq. (12) holds for the heavy element region, and as a first approximation, that this same value of c should hold for fission in the lighter elements. The value of c so obtained is 0.145 $Mev^{1/2}$, and we have

$$\log \Gamma_f/\Gamma_n = \log K + \frac{B_n - B_f}{\sqrt{E_x}\ 0.334} . \qquad (21)$$

B. The Existing Cross-Section Data for Low-Energy Light-Element Fission.

Figure 3 represents almost all the experimental data available for light-element fission in this energy range. Figure3 is from the work of Fairhall (obtained by private communication). These are the original data used in the curves in Reference[2], in the excitation curves in Reference [1], and in the Γ_f/Γ_n curves of References[10] and[8].* Figure 4 is from Griffioen[15] and furnishes additional data for two of the lightest nuclei studied, tantalum and rhenium. It is to be noticed that the rhenium cross-sections from Griffioen are significantly higher than those of Fairhall (Figure 3).

Figures 5a and 5b show Leachman's data on the neutron fission of Ra^{226},[7] which provide the most complete analysis available of a single excitation function. Figure 5a shows the actual points and Figure 5b shows a possible curve through these points (Ref.8).

Table 1 gives some additional numerical values. It lists only data that do not appear on Figures 3 through 5. There are additional points from Bi^{209} (α, f) and Bi^{209} (d, f) obtained by Gilmore[17]. A comparison of these figures with Fairhall's Bi points (Figure 3), again shows that there is fair

*In a recent development, Nicholson[16] has duplicated some of the measurements by Fairhall on Bi, Pb, and Au, using counting methods. His cross-sections are fairly close to those of Fairhall at high excitation but are significantly lower at the lower energies. Nicholson estimates thresholds by fitting his excitation functions to the more exact Γ_f/Γ_n expressions, of which 15 to 17 are approximations. His values are of the same magnitude but somewhat lower than those obtained by the above approach.

Table I

Numerical data on low-energy fission cross sections in light elements*

Target	Projectile	Compound nucleus	E_x (Mev)	Total σ_f (cm^2)	Reference
Bi^{209}	d	Po^{211}	20.5	$9 \cdot 10^{-31}$ a	17
			24	$3.2 \cdot 10^{-30}$ a	
			26	$1.0 \cdot 10^{-29}$ a	
			30	$4.0 \cdot 10^{-29}$ a	
Bi^{209}	d	Po^{211}	22.4±.5	$6.7 \pm 6.7 \cdot 10^{-29}$ b	20
			27.2±1.0	$1.7 \pm 1.7 \cdot 10^{-27}$	
Ra^{226}	d	Ac^{228}	30	$5 \cdot 10^{-26}$	1
Ra^{226}	p	Ac^{227}	16.5	$\sim 3.3 \cdot 10^{-29}$	21
			18.5	$2 \pm 1 \cdot 10^{-27}$	
Au^{197}	α	Tl^{201}	42.9	$9.3 \cdot 10^{-30}$ a	17
			33.1	$3.1 \cdot 10^{-31}$ a	
Bi^{209}	α	At^{213}	38.0	$6.3 \cdot 10^{-27}$ c	
			29.0	$2.0 \cdot 10^{-28}$ c	
			21.1	$4.7 \cdot 10^{-30}$ c	
			15.0	$3.3 \cdot 10^{-31}$ c	

Yields estimated from mass-yield curves in References (1) and (2).

a. Using estimated yield of 10% for Mo^{99}.

b. Assuming 6% yield for Y^{93}.

c. Assuming 6% yield for Ag^{111}.

* Not given in Figures 3, 4, and 5

agreement at the high energies but considerable disagreement at lower energies for the alpha points, although the deuteron points are fairly close. The data on the alpha fission of gold are in considerable disagreement with Fairhall's.

The most important conclusion to be drawn is that there just are not enough data on any one nuclide to determine the validity of any theoretical or semi-empirical interpretation or calculation; nor is there sufficient agreement between data from different sources to allow one to expect any more than rough estimates of thresholds by the method of IIA.

C. Calculation of Thresholds

Figure 6 shows a plot of log Γ_f/Γ_n vs. $1/\sqrt{E_x}$ for the data of Part B. Many of the curves are taken directly from Fairhall[2]. The curves for Bi, Re, and Ta were calculated directly by Eq. (12). The Ra curve was taken from Vandenbosch and Huizenga[8].

By using the curves from Figure 6, thresholds were calculated from Eq. (21) from what were estimated to be the "best" slopes. In the cases (Bi and Re) in which different sets of data were available, a threshold was estimated for each. Neutron binding energies were obtained from (18) or (19) or were estimated. The results are shown in Table II. Thresholds calculated by use of Halpern's temperature expression (Eq. (10)) are also listed. It is to be noted that these are quite high compared with those estimated from the liquid-drop calculation in Part III.

Since only one W point was available and since the Ta points were much too close to estimate a slope, an attempt was made to calculate B_f directly from Eq. (21) for these cases, using an intercept estimated from Figure 6 of log K = 3.5. This is considerably different from Halpern's value of 0.6 for the pre-exponential constant. For comparison, the W threshold was calculated from Halpern's original formula, Eq. (17). A calculation of the former kind seemed justified, since there appeared to be some convergence in the light element Γ_f/Γ_n curves (if one considers Ra to be a curve of a different family!), which may be taken as evidence that these curves have a roughly common intercept. Both calculations give reasonable although somewhat different results. (See Table II). This seems to confirm the comment of Halpern[10] that both direct calculation and slope measurement of such curves as Figure 6 lead to reasonable threshold estimates. He sees this as evidence that the assumptions behind Eqs. (15) and (16) are not completely without basis.

Table II

Comparison of "calculated" thresholds with those estimated from Γ_f/Γ_n plot (in Mev)

Alpha target	Compound nucleus	Liquid-drop calculation	Taken from Γ_f/Γ_n (slopes)	Halpern[10]
Ra^{226}	Ra^{227}	7.68	9.00	15.9[g]
Pb^{207}	Po^{211}	21.1	17.4	
Pb^{204}	Po^{208}	18.1	22.46	22[h]
Pb^{208}	Po^{212}	21.1	17.0	34[g]
Pb^{206}	Po^{210}	21.3	21.9	
Tl	Bi	23.3[i] 26.7[i]	26	58.5[g]
Hg	Pb	20	25	2.8[h]
Au	Tl^{201}	25.6	25.6	
Pt	Hg	24.66[i] 27.36[i]	24	32[h]
Ir	Au	27.9	22	
Os	Pt	23.3[i] 30.7	21	
Re	Ir	27.6	34[a] 23[b]	
W	Os	29.3[i] 32.5[i]	40[c] 28[d]	
Bi	At	15.6	16[e] 24.5[f]	
Ta	Re	30	29[d]	

[a]Fairhall's Re data.
[b]Griffioen's Re data.
[c]Halpern's formula: $0.6\ e^{+\Delta/T}$, Eq. (17)
[d]Calculated directly from points using Eq. (20) and log K = 3.5.
[e]Fairhall's data.
[f]Gilmore's data.
[g]Calculated from Γ_f/Γ_n slopes by using $T^2 = E_x/7.5$
[h]Quoted values Ref. 10
[i]Multiple values refer to different isotopes (see Table III).

The most striking feature of Figure 6 is the gap between the light-element curves and the Ra curves. This is another reflection of the change in the fission process in the elements below Ra.

Can the observed Γ_f/Γ_n data be fitted by an equation similar to (19)? From the amount of data available it is difficult to formulate a unique answer. The curves for Au^{197}, Hg, Pb^{204}, and Pb^{207} seem to fall on fairly straight lines, but those of Pb^{206} and Pb^{208} are more irregular. All the curves tend upward at lower energies. The lack of agreement in the results of various investigators makes any decision on this point quite uncertain.

Whether the expected increase in steepness (more negative slopes) occurs as we go to lighter elements — reflecting the increase in fission thresholds — occurs is also difficult to determine, since the curves for the lower elements have but one or two points on them.

III. SEMIEMPIRICAL ESTIMATION OF THRESHOLDS FROM THE LIQUID-DROP MODEL

In conjunction with our earlier definition of the threshold, we can write

$$\text{Threshold} = \text{saddle-point mass} - \text{ground-state mass}. \qquad (22)$$

In this discussion, experimental ground-state masses are used, whereas the saddle-point mass is estimated theoretically but is normalized by use of Leachman's data (Figure 5) for Ra.

It is shown in the original treatment of fission by the liquid-drop model,[13] and also by Swiatecki,[22] when (1-x) is small compared with 1, the saddle-point mass is proportional to $(1-x)^3$. The value near x = 0 is also known, since the critical shape there is known to be two spheres in contact. As was mentioned earlier (page 5), calculations utilizing various models for the critical shape have indicated that there is not just a gradual deviation from the $(1-x)^3$ law to reach the proper intercept at x = 0, but that the curve takes on an entirely different form. Furthermore, these calculations have suggested that a quadratic representation of the saddle-point mass curve in this range of x might not be too bad an approximation. We can write

$$\xi = c + bx + ax^2 \quad , \qquad (23)$$

where a, b, and c are constants, and

$$\xi = \frac{\text{saddle-point energy}}{\text{original surface energy}} = \frac{E_{th}}{E_s(0)} \quad . \qquad (24)$$

In this treatment the undistorted shape is considered sperical, with $E_s^o = 4\pi r_o^2 A^{2/3}$, $\sigma = 1.912 \times 10^{-2} A^{2/3}$ amu $= 17.80 A^{2/3}$ Mev. Let B_s be the factor by which the surface energy is changed upon deformation from the equilibrium shape. Let B_c be the factor by which the Coulomb energy is changed upon deformation, then the total change in energy of the deformed nucleus is

$$E_{th} = E_s^o (B_s-1) + E_c^o (B_c-1) = E_s^o \left[(B_s-1) + 2x(B_c-1)\right] , \qquad (25)$$

where x is the fissionability parameter = (charge)^2/10 x volume x (surface tension) =

$$\frac{Z^2/A}{(Z^2/A)_0} = E_c^o/2E_s^o ;$$

$$\xi = \frac{E_{th}}{E_s^o} = \left[(B_s-1) + 2x (B_c-1)\right] . \qquad (26)$$

One can evaluate c and b theoretically by noting that they are, respectively, the value of ξ and the first derivative of ξ evaluated at x = 0. Bohr and Wheeler[13] have evaluated ξ (0) as 0.259921 by considering two spheres in contact. An expression for the first derivative may be simply obtained, since ξ is usually considered to be a function of shape and x only:

$$\frac{d\xi}{dx} = \left(\frac{\partial\xi}{\partial(\text{shape})}\right)_x \frac{d(\text{shape})}{dx} + \left(\frac{\partial\xi}{dx}\right)_{\text{shape}} , \qquad (27)$$

but since we are considering a series of equilibrium shapes, we can write

$$\left(\frac{\partial\xi}{\partial(\text{shape})}\right)_x = 0 , \qquad (28)$$

and

$$\left(\frac{d\xi}{dx}\right)_{x=0} = \left(\frac{\partial\xi}{\partial x}\right)_{\substack{\text{shape} \\ x = 0}} = 2(B_c-1)_{x=0} . \qquad (29)$$

Bohr and Wheeler[13] have evaluated this initial slope (although by a different method) as -0.215112.

It was decided to leave a as an adjustable parameter to be normalized by means of an estimate of the Ra^{227} threshold from Figure 5. Leachman's measurements on Ra^{226} [7] (Figure 5) were carried to sufficiently low cross-sections

to enable a threshold estimate for Ra^{227} to be made. From Figure 5 an average of the lower three points was taken for the neutron energy associated with the fission threshold. The neutron binding energy in Ra^{226} is 4.81 mmu and 4.01 Mev must be added owing to the difference in the actual mass of Ra^{227} and the smooth reference surface from which ξ is measured. This gave a value of E_{th} of 12.37 mmu or $\xi = 0.016179$. Since we have $x = 0.6804$ for Ra^{227}, using $(Z^2/A)_o = 50.12$, we may calculate a as -0.21037. Therefore,

$$\xi \cong 0.259921 - 0.215112x - 0.21037\, x^2;\ E_{th} = \xi\, E_s^{(0)}. \qquad (30)$$

This normalization is admittedly rough, but as soon as good threshold data in this region are available, renormalization and possibly an empirical evaluation of the coefficient of x will be a simple matter. Ra also had disadvantages as a normalization point in that it may lie too close to the $(1-x)^3$ region where Eq. (23) would not be expected to hold.

Ground State Masses

Since the values of E_{th} calculated by Eq. (30) are relative to a smooth liquid-drop mass surface, to obtain the threshold relative to the actual masses, it is necessary to add the difference between the liquid-drop and the observed ground-state masses:

$$B_f = E_s^0\ \xi + \Delta\ , \qquad (31)$$

where

$$\Delta = M_{liquid\text{-}drop} - M_{exp.} \qquad (32)$$

Green's values for liquid-drop masses (without the δ term) were used along with a σ term:

$$\delta \begin{cases} = 12.03/A^{1/2} & \text{odd-odd nuclei} \\ = 0.09 & \text{odd-Z, even-A} \\ = -0.09 & \text{even-Z, odd-A} \\ = -12.03/A^{1/2} & \text{even-even} \end{cases} \qquad (33)$$

The experimental masses given by Foreman and Seaborg[18] were used for elements above lead; whereas those of Wapstra[19] were used for the remainder. A systematic difference of 0.24 mmu was found between these two compilations, and it was necessary to subtract this much from Wapstra's values. Table III gives the results of the above calculation down to Sn compound nuclei.

Figure 7 shows a plot of the threshold calculated by Eq. (31) vs Z^2/A. There is a large amount of scatter in the points due to: (a) fluctuations in the ground-state masses, and (b) the fact that the calculated threshold, even when referred to the smooth mass surface, is not a smooth function of any one parameter. ξ contains one term dependent on x and a second on x^2, therefore, when ξ is multiplied by the surface energy to give the threshold in some energy unit, the resulting expression has one term proportional to $Z^2/A^{1/3}$ and a second to $Z^4/A^{4/3}$ and cannot be represented adequately by any one of these parameters. However, the main features of the results can still be seen in Figure 8. As expected, a sharp increase in the threshold values in Eq. (31) relative to the experimental points for the heavy elements occurs in the region of Ra. This may be attributed to the dip in the ground-state masses relative to the smooth mass surface near the double closed shell of Pb^{208}. Below this the thresholds increase more slowly owing to the increase in ξ as x decreases. Although it is not evident in Figure 8, the threshold values are beginning to level out at the lower values of x because the decrease in $A^{2/3}$ tends to oppose the threshold increase caused by the decrease in x.

CONCLUSION

Table II shows a comparison of the results of the liquid-drop calculations with the values estimated from the Γ_f/Γ_n slopes. The agreement is surprisingly good considering the crudeness and complete independence of both methods, and the incompleteness and seeming lack of reproducibility of the data; however, there is still much to be desired.

The thresholds calculated from the liquid-drop are in much better agreement with the values obtained from the Γ_f/Γ_n slopes when a temperature constant of 0.145 is used rather than Halpern's temperature expression, Eq. (18).

Figure 8 shows a plot of B_f-B_n calculated by using the liquid-drop values of Eq. (32) vs the observed values of Γ_f/Γ_n. Although the points are scattered, the plot is sufficient to indicate the sharp difference between the

Table III

Threshold Values Calculated From Eq. (31)

Target	Compound nucleus	B_f (Mev)	Target	Compound nucleus	B_f (Mev)
Bi^{209}	At^{213}	15.62	Lu^{176}	Ta^{180}	35.8
Pb^{204}	Po^{208}	18.07	Yb^{176}	Hf^{180}	39.3
Pb^{206}	Po^{210}	21.3	Yb^{174}	Hf^{178}	35.8
Pb^{207}	Po^{211}	21.1	Yb^{172}	Hf^{176}	34.0
Pb^{208}	Po^{212}	21.13	Er^{168}	Yb^{172}	44.5
Tl^{203}	Bi^{207}	23.35	Dy^{164}	Er^{168}	43.8
Tl^{205}	Bi^{209}	26.70	Gd^{160}	Dy^{164}	46.9
Hg^{198}	Pb^{202}	19.79	Gd^{158}	Dy^{162}	44.8
Au^{197}	Tl^{201}	25.61	Gd^{156}	Dy^{160}	41.2
Pt^{194}	Hg^{198}	24.66	Sm^{154}	Gd^{158}	48.0
Pt^{196}	Hg^{200}	27.36	Sm^{152}	Gd^{156}	44.7
Ir^{193}	Au^{197}	27.86	Nd^{144}	Sm^{148}	45.4
Os^{188}	Pt^{192}	23.25	Nd^{142}	Sm^{146}	45.4
Os^{192}	Pt^{196}	30.68	Ce^{140}	Nd^{144}	51.0
Re^{187}	Ir^{191}	27.60	Ba^{138}	Ce^{142}	57.5
W^{182}	Os^{186}	29.30	Xe^{134}	Ba^{138}	62.6
W^{186}	Os^{190}	32.47	I^{127}	Cs^{131}	54.0
Hf^{176}	W^{180}	30.66	Te^{130}	Xe^{134}	65.2
Hf^{180}	W^{184}	36.05	Te^{128}	Xe^{132}	61.0
Lu^{175}	Ta^{179}	35.43	Sb^{123}	I^{127}	56.6
Yb^{176}	Hf^{180}	41.13	Sb^{125}	I^{129}	53.5
Er^{170}	Yb^{174}	54.48	Sn^{120}	Te^{124}	56.5
Hf^{180}	W^{184}	36.1	Sn^{118}	Te^{122}	53.7
Hf^{179}	W^{183}	35.1	In^{113}	Sb^{117}	51.4
Hf^{178}	W^{182}	33.5	Cd^{114}	Sn^{118}	56.4

heavier and the lighter elements. The light-element points represent an excitation energy of about 39 Mev or about 10 to 20 Mev above the barrier. The heavy-element points were taken from Reference 8, and correspond to an excitation energy of 8 to 12 Mev, but it was shown[8] that the Γ_f/Γ_n dependence on energy is slight for the heavier elements, and it is on this basis that the comparison of the two sets of points on Figure 8 can be made. This is a further indication of the change in the trends of the fission process for the elements below Ra. According to Figure 8, Ra itself falls more in line with the trends in the light elements.

Figure 9 shows a comparison of values of ξ obtained from Eq. (30) with those obtained from saddle-point heights of potential energy-deformation surfaces as calculated by Swiatecki[5]. These calculations represent the most exact treatment of the liquid-drop carried out so far, and it is pleasing to see that such a simple expression as Eq. (30) is in good agreement with them.

The next step seems to be experimental. More complete data, of as high precision as possible are needed if we are to observe the threshold effect as discussed earlier. The feasibility of carrying out these measurements will be the next step in this research program.

ACKNOWLEDGMENT

Thanks are due to Professor J.A. Wheeler, who, through his Physics-244 course, provided the stimulus for the writing of the original draft of this paper.

The aid of Dr. W.J. Swiatecki, who provided the original ideas and many extremely valuable discussions, was a primary factor in the completion of this work.

APPENDIX

Although they are not immediately connected with the threshold problems, it might be interesting to see if the trends of Γ_f/Γ_n with A and Z^2/A at constant excitation as observed by Vandenbosch and Huizenga[8] continued in the lighter elements (Figures 10, 11). These curves are qualitatively the same as those observed by Vandenbosch and Huizenga for the heavier elements. The heavy-element curves for constant Z seem to form a family of curves at about right angles to the main trends. The only light element for which several isotopes have been studied is Pb and a strikingly similar effect is observed. The trend is for Γ_f/Γ_n to decrease as A increases for constant Z. Vandenbosch's explanation for this is that, (a) neutron binding energies decrease as A increases, making it less difficult to evaporate a neutron, and (b), Z^2/A decreases as A increases. That all the points fall roughly in a common band when plotted vs Z^2/A (Figure 10) gives further weight to the latter explanation.

Vandenbosch and Huizenga note that their curves seem to show no odd-even effects. This is likewise found in Figures 10 and 11 except the Pb^{207} and Pb^{206} points are reversed from what would be expected. The explanation offered by Vandenbosch and Huizenga is that even-even nuclei have a larger neutron binding energy, which tends to decrease Γ_n, however, the odd-A nucleus formed after evaporation of a neutron would have a larger level density, thus the cancellation of these two factors should leave Γ_n roughly insensitive to odd-even effects. One might also argue from the idea that Γ_f is related to the ratio of the available phase-space volume at the saddle to the density of states below the saddle point and that perhaps this ratio is independent of odd-even effects.

A more explicit comparison of the heavy and light elements is shown in Figure 12, in which points for compound nuclei between Th and Fm have been taken from Vandenbosch and Huizenga[8]. The trend seems to be quite regular and this seems to be one case in which fission properties of the light elements are just the extrapolation of those of the heavy elements, i. e., the transition to the light elements is smooth when viewed in this way. The remarks concerning excitation energy (pp. 28 and 32) hold for this plot also.

REFERENCES

1. A. W. Fairhall, Second United Nations International Conference on the Peaceful Uses of Atomic Energy, Geneva, 1958. Vol. 15, Paper/688.

2. A. W. Fairhall and E. F. Neuzil, Cyclotron Research, University of Washington, Seattle, 1959. p. 19.

3. R. B. Leachman, The Fission Process, Mechanisms and Data, Second United Nations International Conference on the Peaceful Uses of Atomic Energy, Geneva, 1958. Vol. 15, Paper P/2467.

4. S. Frankel and N. Metropolis, Phys. Rev. 72, 914 (1947).

5. Wladyslaw J. Swiatecki, Lawrence Radiation Laboratory, Berkeley, California, private communication.

6 J. D. Jackson, Proceedings of the Symposium on the Physics of Fission, Chalk River Symposium, 1956, CRP-642A, p. 125.

7. R. A. Nobles and R. B. Leachman, Nuclear Phys. 5. 211 (1958).

8. R. Vandenbosch and J. R. Huizenga, Second United Nations International Conference on Peaceful Uses of Atomic Energy, Geneva, 1958. Vol. 15, Paper/688.

9. Wladyslaw J. Swiatecki, Deformation Energy of a Charged Drop. III, UCRL-3991, May 1958.

10. I. Halpern, Ann. Revs. Nuclear Sci. 9, (1959).

11. R. Vandenbosch and Glenn T. Seaborg, Phys. Rev. 110, 507 (1958).

12. Y. Fujimoto and Y. Yamaguchi, Progr. Theoret. Phys. (Kyoto) 5, 76 (1950).

13. N. Bohr and J. A. Wheeler, Phys. Rev. 56, 426 (1939).

14. J. R. Huizenga, Nuclear Reactions, Vol. II (North Holland Publishing Co., Amsterdam, in press).

15. R. Griffioen, The Low Energy Fission of Rhenium and Tantalum (Thesis), Purdue University, 1960.

16. W. J. Nicholson, Fission Barrier Heights in Light Elements (Thesis), University of Washington, Seattle, 1960.

17. John T. Gilmore (Lawrence Radiation Laboratory, Berkeley, California), private communication.

18. Bruce M. Foreman and Glenn T. Seaborg, Nuclear Thermodynamics of the Heaviest Elements, UCRL-8015 (rev), Jan. 1958.

19. A.H. Wapstra, Handbuch der Physik, Vol. 38, Part I., p.1.
20. A.W. Fairhall, Phys. Rev. 102, 1335 (1956).
21. A.W. Fairhall and R.C. Jensen, Phys. Rev. 109, 942 (1958).
22. Wladyslaw J. Swiatecki, Phys. Rev. 101, 651 (1956).

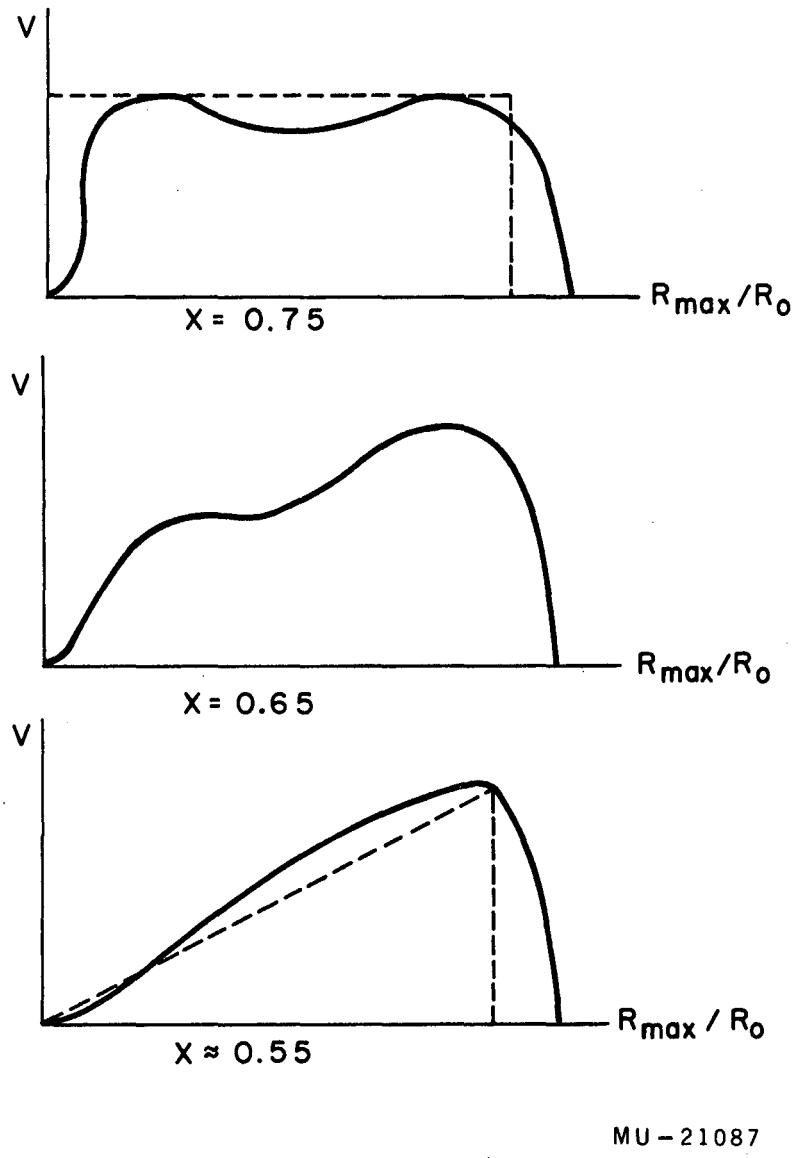

Fig. 1. Fission barrier based on the liquid-drop calculation from References 4, 5 and 9.

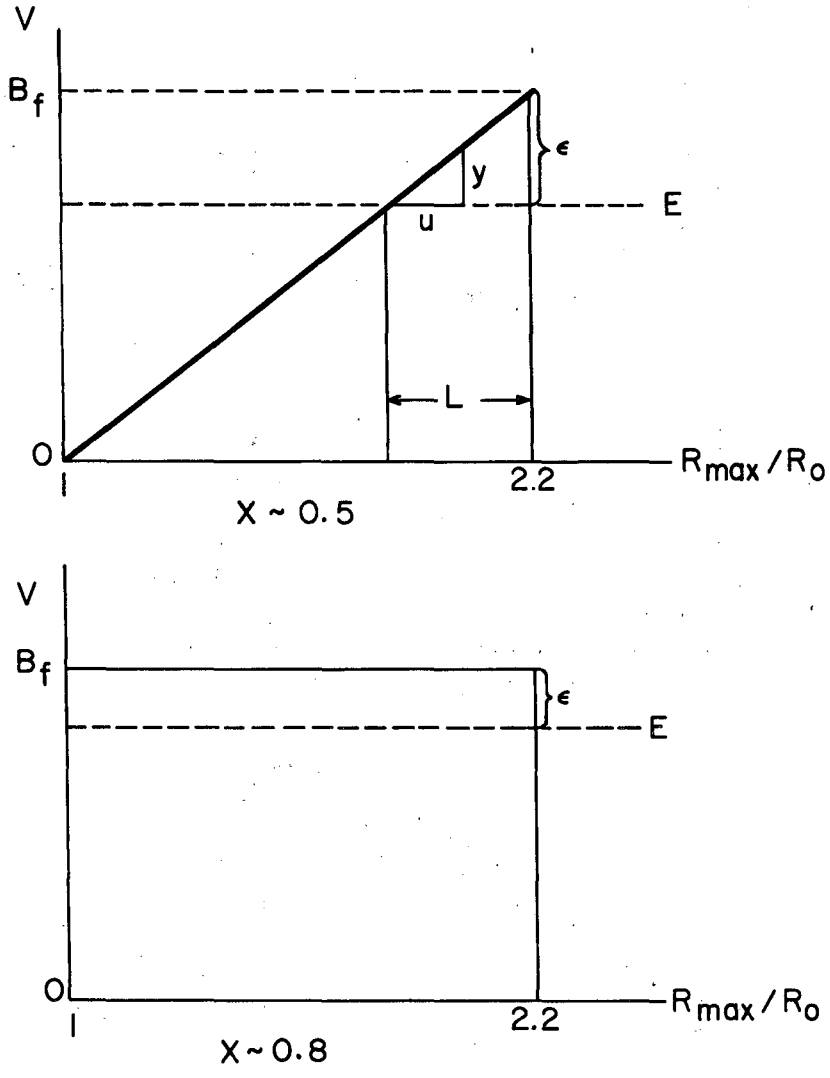

MU-21085

Fig. 2. Idealization of the actual barriers in Figure 1.

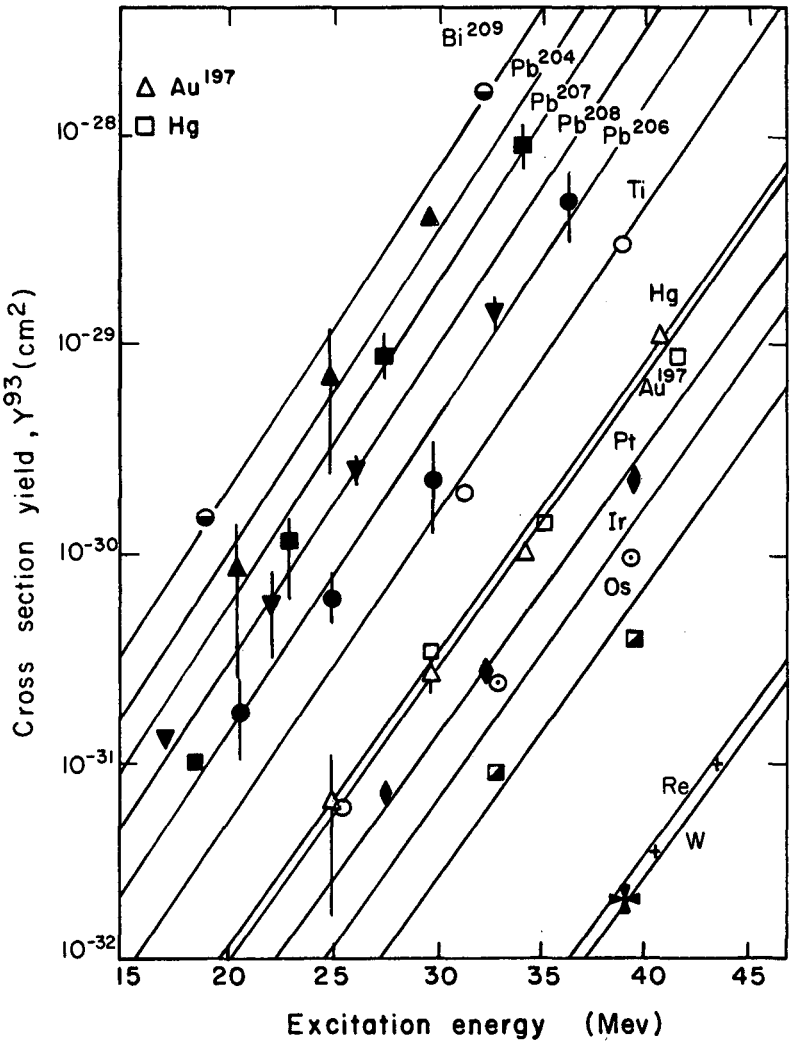

MU-21084

Fig. 3. Fission cross sections from Fairhall.[2]

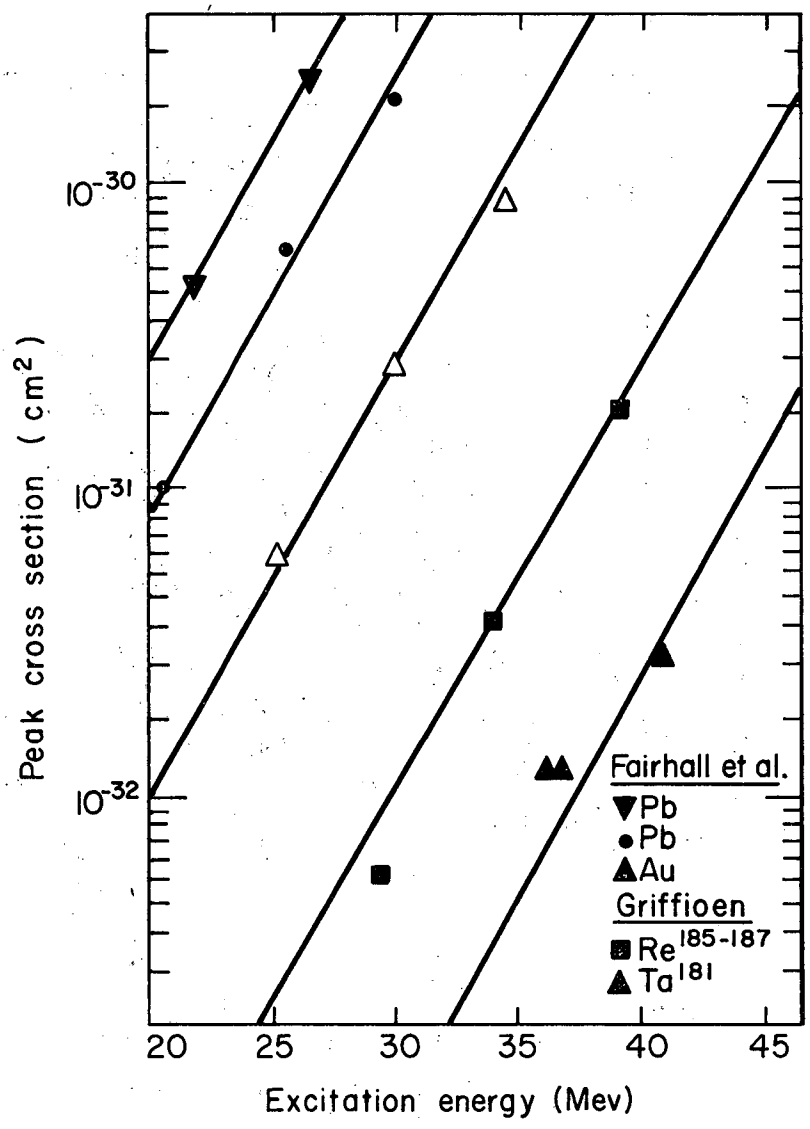

MU-21088

Fig. 4. Fission yields of Re and Ta as measured by Griffioen.[15]

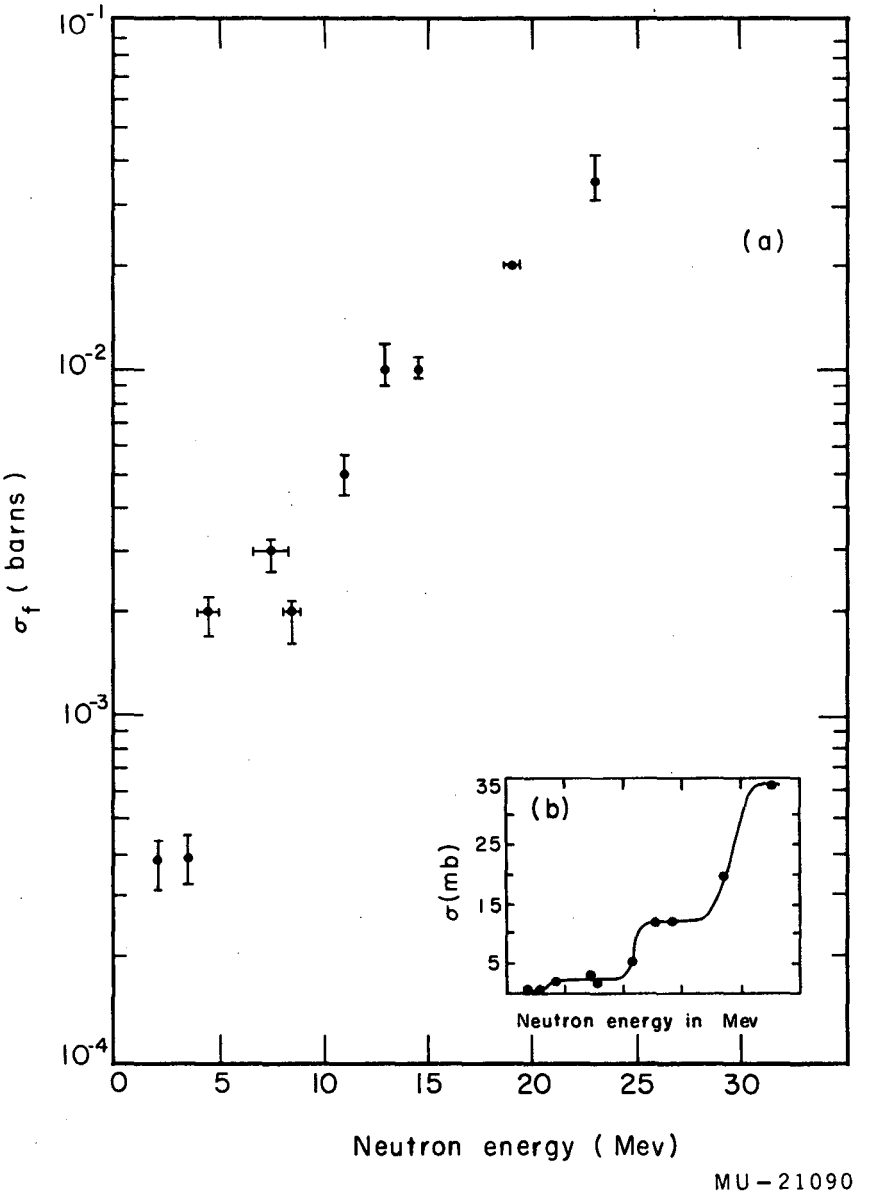

Fig. 5 (a) The total cross section for fission of Ra^{226} by neutrons as measured by Leachman.[7]

Fig. 5 (b) An interpretation of Leachman's data by Vandenbosch[8] emphasizing a threshold character.

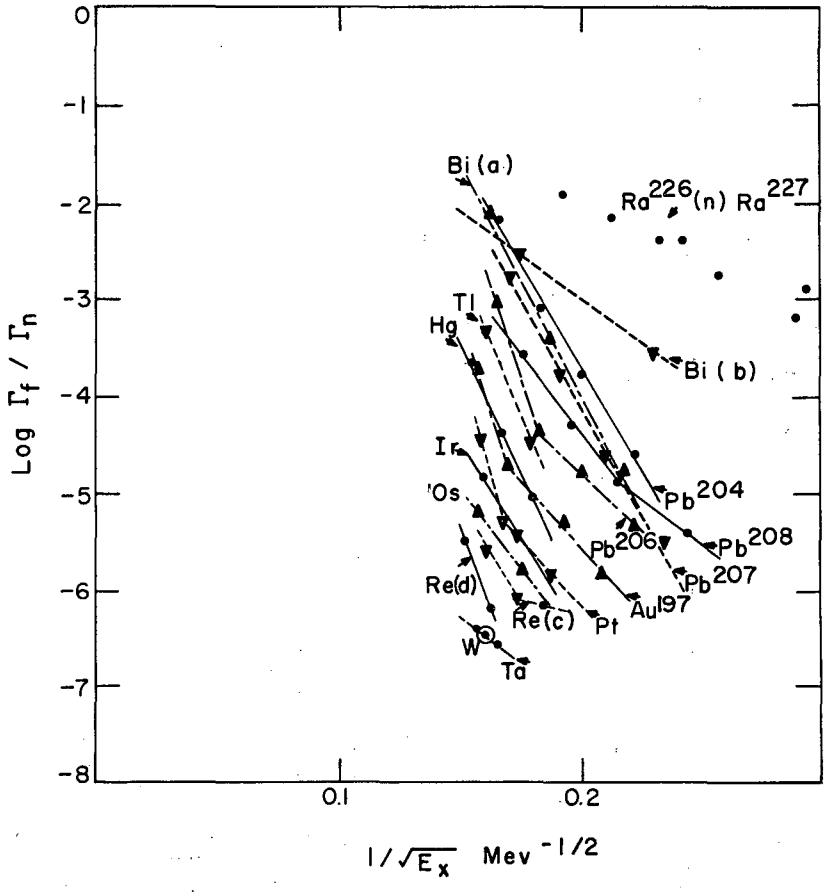

MU-21086

Fig. 6. Plot of log Γ_f/Γ_n vs $E_x^{-1/2}$. Targets of alpha bombardments are elements unless otherwise specified. (a) Fairhall, (b) Gilmore, (c) Griffioen, and (d) Fairhall.

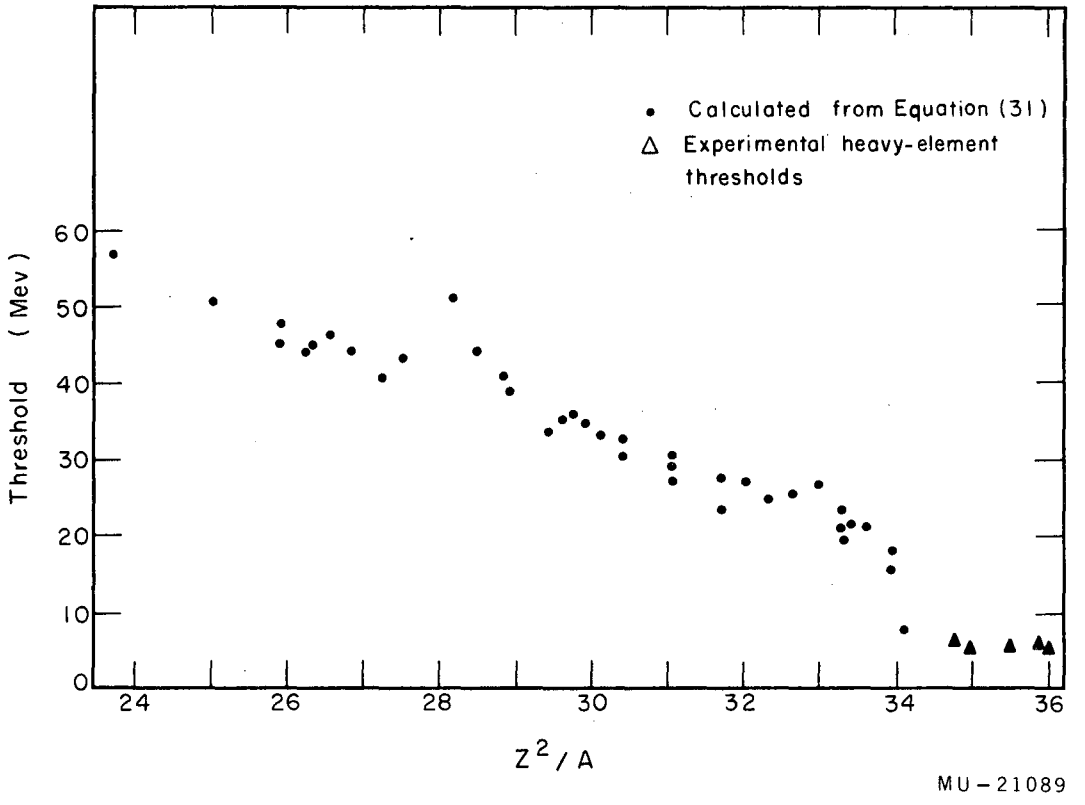

Fig. 7 Fission thresholds as a function of Z^2/A.

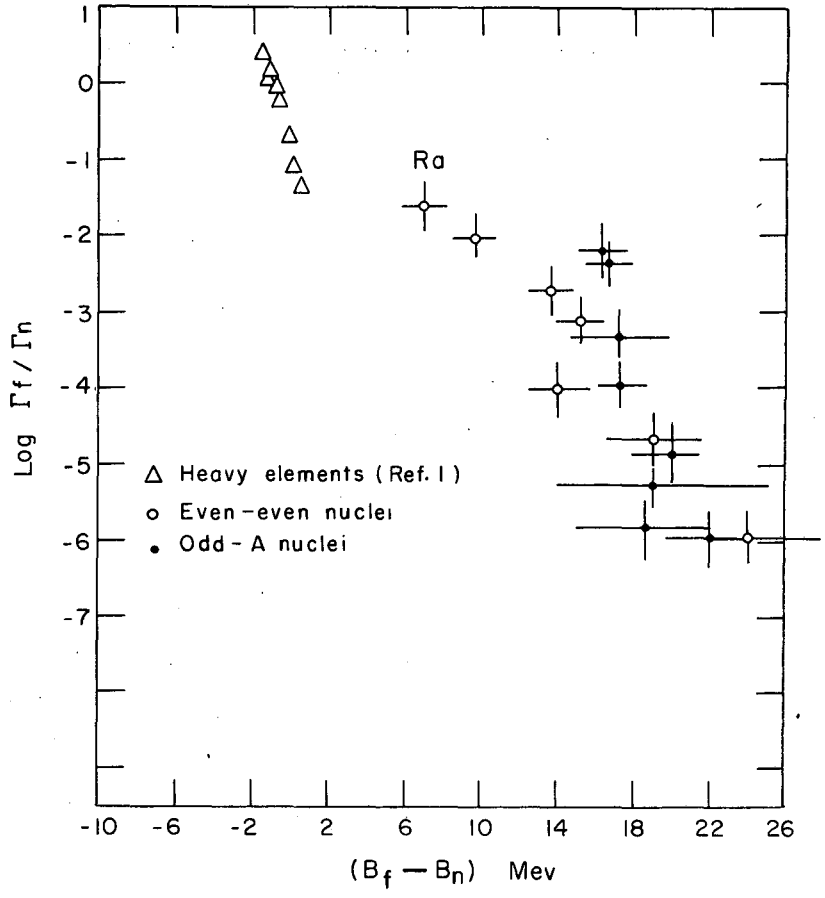

MU-21083

Fig. 8. Plot of log Γ_f/Γ_n vs B_f-B_n for a constant excitation energy. B_f values obtained from liquid-drop calculation (Eq. (31)). Heavy-element points are at an excitation of 10 to 12 Mev. Light-element points are at 39-Mev excitation.

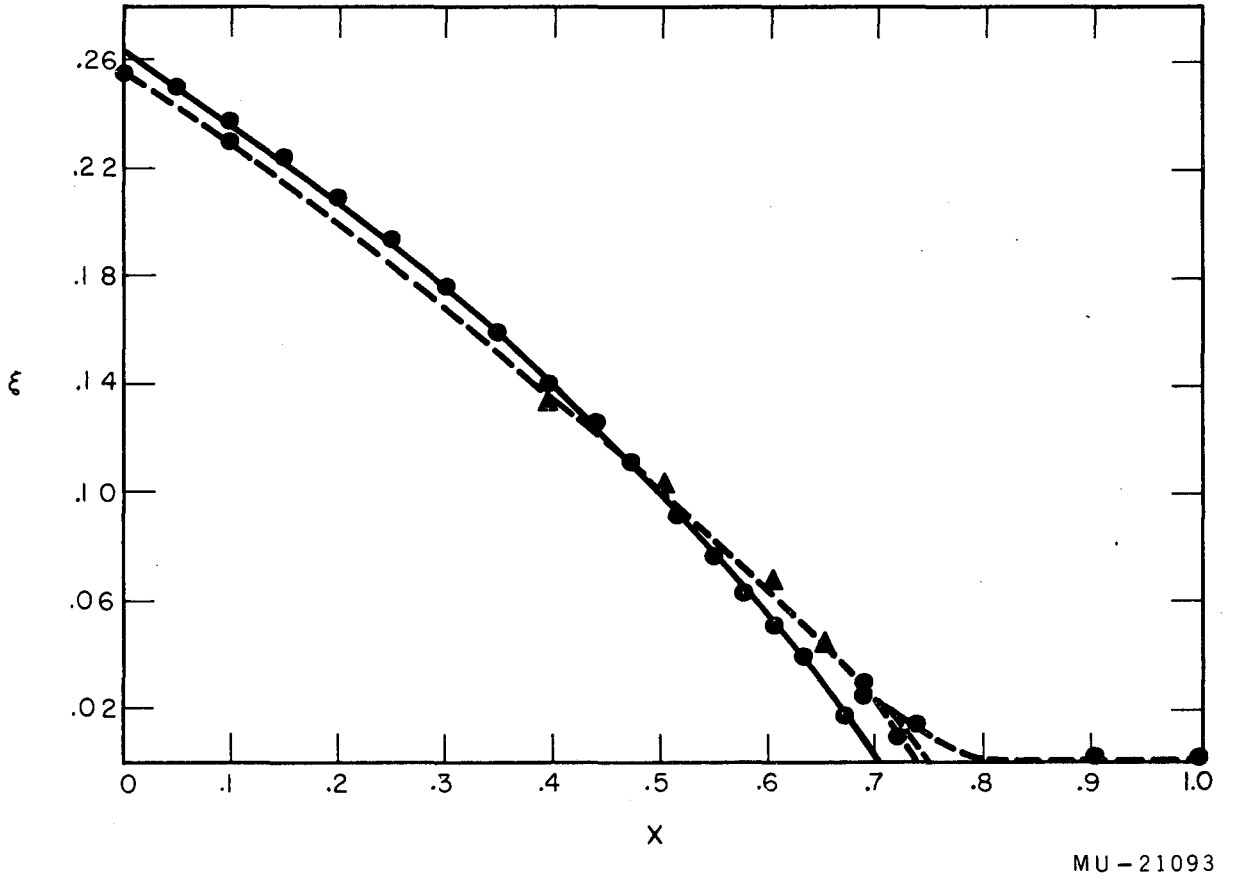

Fig. 9. Comparison of equation (30) with more exact liquid-drop calculations by Swiatecki.[20]

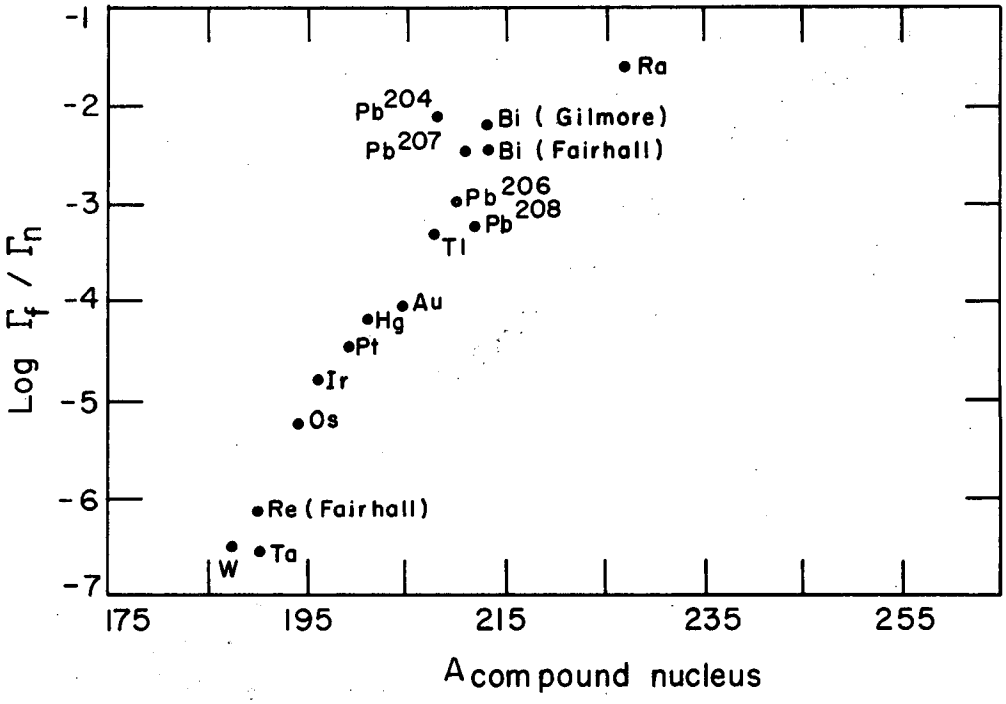

MU-21094

Fig. 10. Plot of log Γ_f/Γ_n vs $A_{\text{compound nucleus}}$ at $E_x^{-1/2} \approx 0.16$ or E_x = 39 Mev. Alpha targets are listed on graph.

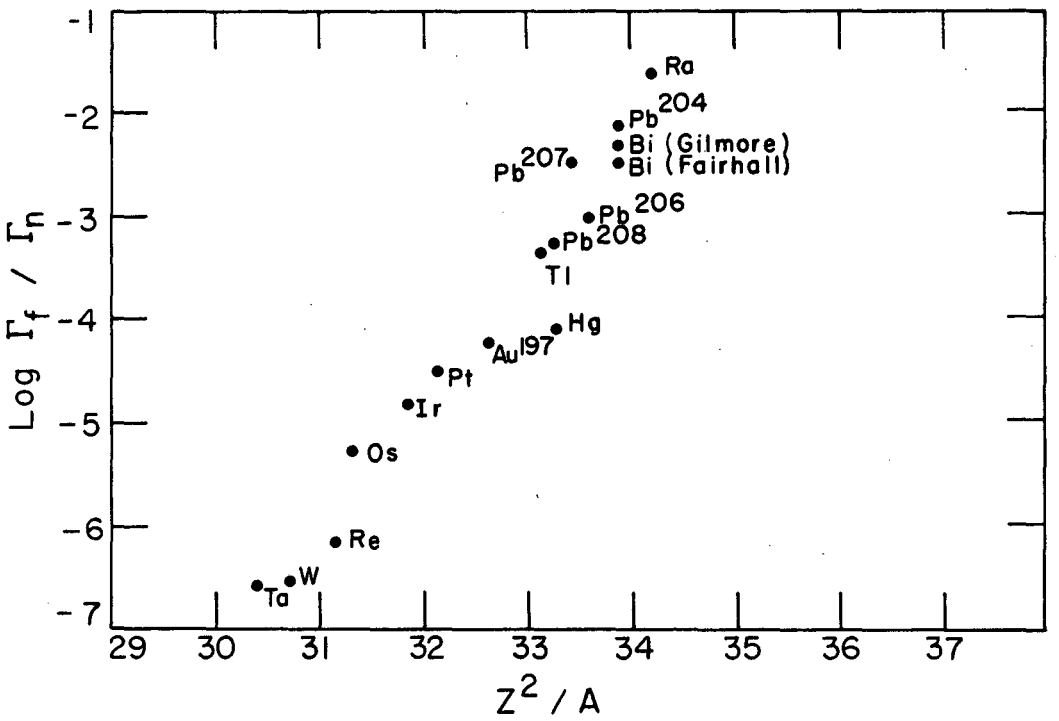

MU-21092

Fig. 11. Plot of log Γ_f/Γ_n vs Z^2/A for E_x = 39 Mev. Alpha targets listed on curve.

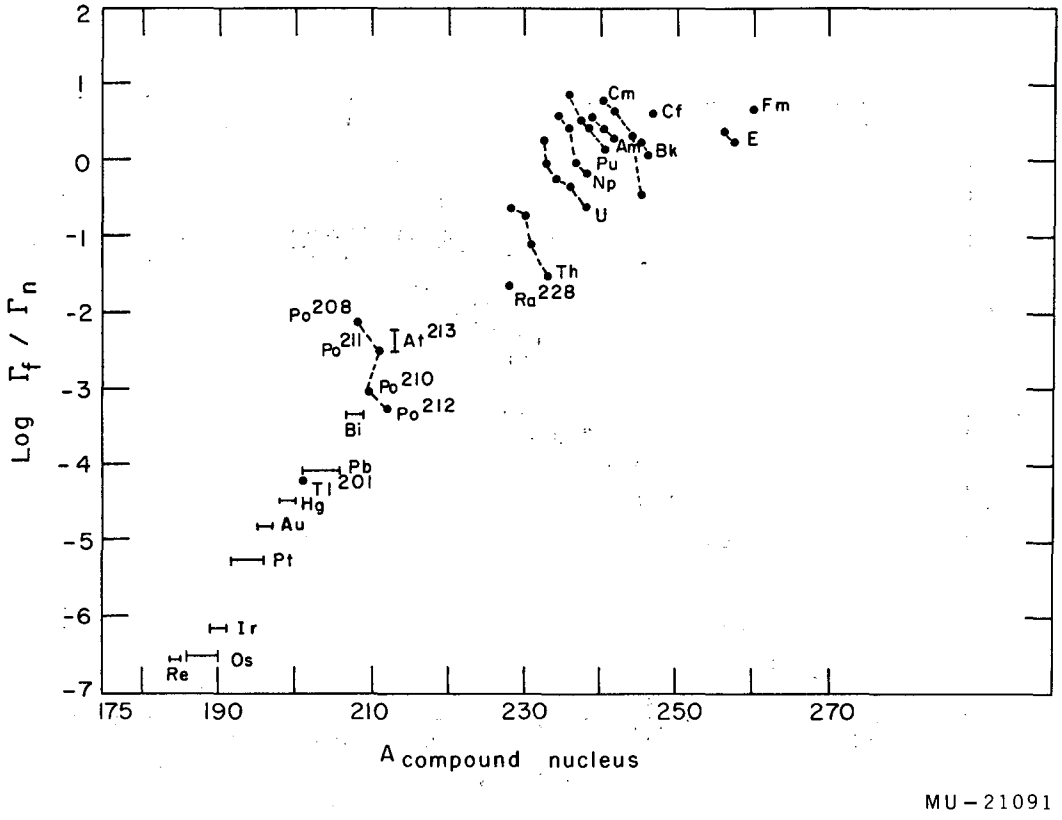

Fig. 12. Comparison of trends in Γ_f / Γ_n vs A for heavy and light elements. Heavy-element data from Vandenbosch and Huizenga[8] at an excitation of 10 to 12 Mev. Light-element data same as that in Fig. 10. Points are labeled according to compound nuclei.

This report was prepared as an account of Government sponsored work. Neither the United States, nor the Commission, nor any person acting on behalf of the Commission:

A. Makes any warranty or representation, expressed or implied, with respect to the accuracy, completeness, or usefulness of the information contained in this report, or that the use of any information, apparatus, method, or process disclosed in this report may not infringe privately owned rights; or

B. Assumes any liabilities with respect to the use of, or for damages resulting from the use of any information, apparatus, method, or process disclosed in this report.

As used in the above, "person acting on behalf of the Commission" includes any employee or contractor of the Commission, or employee of such contractor, to the extent that such employee or contractor of the Commission, or employee of such contractor prepares, disseminates, or provides access to, any information pursuant to his employment or contract with the Commission, or his employment with such contractor.